



# **A New Formulation to Calculate Effective Tension in Large Pipeline Free Spans**

**Gabriel Nascimento<sup>1\*</sup> and Nelson Szilard<sup>1</sup>**

<sup>1</sup>*Federal Fluminense University, Rua Passos da Patria 156, Niterói/RJ – 24210330, Brazil.*

## **Authors' contributions**

*This work was carried out in collaboration between both authors. Author NS designed the study matter as the doctoral supervisor of the first author, managed the work and wrote most of the manuscript. Author GN developed the proposed methodology and performed the numerical analysis. Both authors read and approved the final manuscript.*

## **Article Information**

DOI: 10.9734/CJAST/2018/39377

### Editor(s):

(1) Elena Lanchares Sancho, Professor, Department of Mechanical Engineering, University of Zaragoza, Zaragoza, Spain.

### Reviewers:

(1) Chis Timur Vasile, Ovidius University, Romania.  
(2) Wuyi Wan, College of Civil Engineering and Architecture, Zhejiang University, China.  
Complete Peer review History: <http://www.sciencedomain.org/review-history/23855>

**Method Article**

**Received 14<sup>th</sup> January 2018**  
**Accepted 19<sup>th</sup> March 2018**  
**Published 27<sup>th</sup> March 2018**

## **ABSTRACT**

Since the 70's, when offshore oil exploitation advanced, submarine pipeline design has been the subject of many researcher studies. Pipeline free spans are common and frequently assessed. In spite of this, up to this day, there is no simple and specific formula to calculate the effective tension ( $S_{eff}$ ), which takes into account the pipeline sagging in moderate or large span lengths. Therefore, engineers normally apply finite element analyses, even for preliminary evaluations. On the other hand, there are simple formulae to calculate other parameters such as the deflection, the moment and the natural frequency, which require previous knowledge of the  $S_{eff}$  value. In the present contribution, an approximate formula is proposed, in order to solve the beam differential equation for both pinned and fixed end conditions and make it possible to calculate the  $S_{eff}$  value using a straightforward and relatively simple equation, which takes into account the pipeline sagging. The values calculated using the proposed method were compared to numerical results obtained for many different cases, varying the span length and the effective tension. The analysis results showed that the proposed equation is highly accurate for practical conditions and, therefore, may become a useful tool for the assessment of the pipeline free spans.

\*Corresponding author: E-mail: gabrielcn@id.uff.br;

**Keywords:** Pipeline; free span; effective tension; axial force.

## 1. INTRODUCTION

The increase of oil demand has driven the development of structures from onshore to offshore [1], but following this same trend the diminishing availability of oil in shallow water reservoirs pushed engineers to design more facilities in deep and, recently, ultra-deep waters. In addition, longer submarine pipelines are required both because of the longer distances to shore as in order to maximize the number of wells covered by the same platform. As a consequence of this, the number of free spans also increases, caused by seabed imperfections and/or crossings. After the installation, scour pits, induced by environmental current turbulence, can also create free spans or expand the existing ones [2]. On the other hand, the unacceptably increased spans require intervention, increasing costs and extending the execution time. Consequently, the assessment of free spans is a very important and frequent procedure in both design and conservation of submarine pipelines, demanding reliable and easy methodologies.

Free spans are evaluated as horizontal beams supported by their ends with applied loads such as temperature, internal and external pressures, self-weight (of the pipe, content, coating, etc.), wave, current and dynamic forces due to vortex induced vibrations (VIV). The three last of these will not be discussed in this work. The temperature increment  $\Delta T$  acts directly into axial strain  $\varepsilon = \Delta T \cdot \alpha_e$ , where  $\alpha_e$  is the temperature expansion coefficient. Internal and external pressure drives the hoop stress and, consequently, due to the Poisson effect, cause axial stress. In addition, as a second order effect, demonstrated by Palmer and Baldry [3] and after in more details by Sparks [4], internal and external pressure create lateral forces on curved segments, whose behavior can be considered as equivalent to a beam axially loaded by

$$S_{eff} = N_{tr} - p_i A_i + p_e A_e \quad (1)$$

where  $S_{eff}$  is the so-called effective tension,  $N_{tr}$  is the true steel wall axial force,  $p_i$ ,  $p_e$ ,  $A_i$ ,  $A_e$  are the internal and external pressures and cross sections areas, respectively. More discussion can be found in literature about this in [5–7].

For a totally restrained pipe, the code DNV-RP-F105 [8] presents the following formulation:

$$S_{eff} = H_{eff} - \Delta p_i A_i (1 - 2\nu) - A_s E \Delta T \alpha_e \quad (2)$$

where  $H_{eff}$  is the effective tension just after the pipe installation (lay tension),  $\Delta p_i$  is the internal pressure increment,  $\nu$  is the Poisson coefficient,  $A_s$  is the steel cross section area and  $E$  is the Young modulus. The external pressure  $p_e$  is already accounted in  $H_{eff}$ .

However, as mentioned before, Equation (2) is valid only for a totally restrained pipe, which is not the condition of free spans, where sagging causes elongation and increases  $S_{eff}$ . At the same time, according to the Beam Theory,  $S_{eff}$ , together with the self-weight  $q$  (N/m) and section properties, defines the sagging. Therefore, in order to calculate the free span  $S_{eff}$  a Finite Element Analysis (FEA) is normally performed.

The  $S_{eff}$  value is required to calculate the natural frequencies, deflection, true axial force  $N_{tr}$ , and bending moment  $M$  [8]. With  $N_{tr}$  and  $M$ , it is possible to determine the axial stresses in the pipe. The natural frequencies are also important for the dynamic VIV evaluation.

Hobbs [9,10] developed a solution based on Beam Theory for the upheaval buckling of submarine pipelines where, as in free spans, the final position and axial force are directly related and unknown. However, due to the complexity of the equations, the calculation of the final configuration based on a given condition of pressure and temperature require numeric computations.

More recently, Vedeld et al. [11] developed a semi-analytical solution for natural frequencies with remarkable accuracy and, unlike the formulation in [8], with no limitations of span length and deflection. Nevertheless, it still depends on the value of  $S_{eff}$  for the static condition, so he then used an iterative approach to calculate  $S_{eff}$ . Sollund et al. [12] applied the same solution for very short span lengths, with the span length - outer diameter ratio smaller than 30, where sagging can be neglected and  $S_{eff}$  is calculated directly by Equation (2).

The effective tension  $S_{eff}$  is a primary result required for several assessments in free spans. However, there are no direct and accurate solutions known in literature for the  $S_{eff}$  in spans with a considerable length. This work presents an approximate solution with sufficient accuracy,

which engineers can apply in submarine pipeline design, as a reliable and easy tool. Two different conditions will be addressed regarding boundaries: pinned-pinned and fixed-fixed. The soil stiffness at the shoulders will not be considered at this moment.

## 2. PROPOSED SOLUTION

### 2.1 Mathematical Problem

According to the Beam Theory, the behavior of a horizontal beam subjected to axial and transversal uniform loads is described by the differential equation

$$EI \frac{d^4 v}{dx^4} - S_{eff} \frac{d^2 v}{dx^2} + q = 0 \quad (3)$$

where  $I$  is the area moment of inertia,  $E$  is the Young modulus,  $v(x)$  is the vertical displacement,  $x$  is the longitudinal position along the pipe,  $S_{eff}$  is the axial load (positive for tension) and  $q$  is the vertical load per length unit, assumed as the submerged self-weight. For the desired boundary conditions, Equation (3) has different analytical solutions, depending if  $S_{eff}$  is positive (tension), negative (compression) or null.

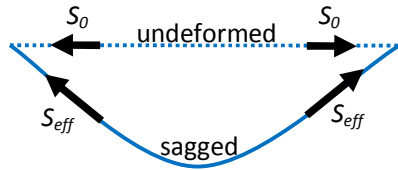


**Fig. 1. Effective tension for undeformed and sagged (buckled) positions**

In free span segments, the sagging causes an elongation of the pipe and thus  $S_{eff}$  increases. Relative to the straight position (undeformed), the post sagging effective tension, assumed constant along span length  $L$ , can be calculated by

$$S_{eff} = S_0 + E A_s \varepsilon_s \quad (4)$$

where  $S_0$  is the undeformed effective tension (Fig. 1), calculated by Equation (2), and  $\varepsilon_s$  is the axial strain due to sagging, derived from

$$\varepsilon_s = (1/L) \int_0^L \left[ \sqrt{1 + (dv/dx)^2} - 1 \right] dx \quad (5)$$

which can be approximated, for small relative displacements, as:

$$\varepsilon_s \cong \frac{1}{2L} \int_0^L \left( \frac{dv}{dx} \right)^2 dx \quad (6)$$

Theoretically, the system of Equations (3), (4) and (6) could be solved in order to calculate  $S_{eff}$  for a given condition of pressure and temperature. However, the solution of Equation (3) depends on the sign of  $S_{eff}$  (positive, negative or null) and is not simple, making it unfeasible for a general mathematical solution.

### 2.2 Solution with an Approximated Displacement Equation

In order to make feasible the derivation of a general solution for the aforementioned problem, an approximated equation for the vertical displacement is used. The expression chosen to take place as the approximate solution of Equation (3) is a fourth degree polynomial, given by Equation (7). The reason for this choice was the good agreement of second and third derivatives with the bending moment and shear force diagrams, respectively, of a beam with a uniform transversal load.

$$\bar{v}(x) = a_4 x^4 + a_3 x^3 + a_2 x^2 + a_1 x + a_0. \quad (7)$$

A relation between the coefficients  $a_i$  can be derived applying the proper boundary conditions (BC's) for each configuration, as shown in Table 1.

**Table 1. Boundary conditions and derived coefficients**

Description	Symbol	Value	
		Pinned-pinned	Fixed-fixed
Deflection	$v(x=0)$	0	0
	$v(x=L)$	0	0
Declination	$dv/dx(x=0)$	$\tan(\varphi_0)$	0
	$dv/dx(x=L)$	$\tan(-\varphi_0)$	0
Moment	$EI d^2v/dx^2(x=0)$	0	$M_0$
	$EI d^2v/dx^2(x=L)$	0	$M_0$
Shear force	$EI d^3v/dx^3(x=0)$	$Q_0$	$Q_0$
	$EI d^3v/dx^3(x=L)$	$-Q_0$	$-Q_0$
Polynomial coefficients	$a_3$	$-2La_4$	$-2La_4$
	$a_2$	0	$L^2a_4$
	$a_1$	$L^3a_4$	0
	$a_0$	0	0

Integrating Equation (3), with symmetric BC's (Table 1), will result in

$$EI \frac{d^3 v}{dx^3} - S_{eff} \frac{dv}{dx} + q \left( x - \frac{L}{2} \right) = 0 \quad (8)$$

and then repeating the same procedure will become

$$EI \frac{d^2 v}{dx^2} - S_{eff} v + \frac{qx}{2} (x - L) - M_0 = 0. \quad (9)$$

The left hand of Equations (8) and (9) are differential operators  $L(f(x))$  equals to 0 for the exact solution, which means  $L(v(x)) = 0$ . For the proposed approximate solution, the result will be

$$L(\bar{v}(x)) = R(x) \quad (10)$$

where  $R(x)$  is a residual, related to the approximation error. In an attempt to reduce the error to a minimum value, the averaged error along the span length will be forced to be zero, which means

$$\int_0^L R(x) dx = 0 \quad (11)$$

Then Equation (11) is applied related to the differential operator  $L(f)$  on Equation (8), for the fixed-fixed condition, or on Equation (9), for the pinned-pinned condition. These different equations were chosen in order to get the best fitting, considering the limitations of the approximate formulation in Equation (7). This procedure will determinate its coefficients as a function of  $S_{eff}$ .

$$a_4 = \frac{-q}{C_7 S_{eff} L^2 + 24EI} \quad (12)$$

where  $C_7$  is derived depending on the condition (Table 2). The value calculated from the described procedure for the fixed-fixed condition was 0.5, however, tests showed that 0.6 gives a better fitting. The other coefficients ( $a_3$  to  $a_0$ ) can be directly calculated from  $a_4$  (Table 1).

Once the deflection function  $v(x)$  is known, by means of its coefficients  $a_i$ , it is possible to calculate the axial strain due to the sagging elongation by means of Equation (6):

$$\varepsilon_s = C_8 (a_4)^2 L^6. \quad (13)$$

$$\frac{S_{eff}}{P_{cr}} = \begin{cases} (-c_Q/2 + \sqrt{c_D})^{1/3} + (-c_Q/2 - \sqrt{c_D})^{1/3} - A_2/(3A_3) ; & \text{if } c_D \geq 0 \\ 2c_R^{1/3} \cos(c_T/3) - A_2/(3A_3) ; & \text{if } c_D < 0 \end{cases} \quad (17)$$

Then, according to the developed methodology,  $S_{eff}$  can be calculated directly from  $S_0$ , which is based on pressure and temperature conditions. The solution basically resorts to solving Equation (17) with its parameters defined in Equations (15) and (16), requiring no further FEA or iterative approach.

**Table 2. Coefficient values**

Coefficient	Value	
	Pinned-pinned	Fixed-fixed
$C_2^*$	1	4
$C_5^*$	1/8	1/12
$C_6^*$	5/384	1/384
$C_7^{**}$	2.4	0.6
$C_8^{**}$	17/70	1/105

\* DNV-RP-F105 [8]

\*\* derived formulation

Combining Equations (4), (12) and (13) will result in the following:

$$A_3 \left(\frac{S_{eff}}{P_{cr}}\right)^3 + A_2 \left(\frac{S_{eff}}{P_{cr}}\right)^2 + A_1 \left(\frac{S_{eff}}{P_{cr}}\right) + A_0 = 0 \quad (14)$$

where  $P_{cr} = C_2 \pi^2 EI/L^2$  is the critical buckling load and

$$\begin{aligned} A_3 &= C_2^3 C_7^2 \\ A_2 &= C_2^2 \left[ C_7 \left(\frac{48}{\pi^2}\right) - C_2 C_7^2 \left(\frac{S_0}{P_{cr}}\right) \right] \\ A_1 &= C_2 \left[ \left(\frac{24}{\pi^2}\right)^2 - C_2 C_7 \left(\frac{48}{\pi^2}\right) \left(\frac{S_0}{P_{cr}}\right) \right] \\ A_0 &= -C_2 \left(\frac{24}{\pi^2}\right)^2 \left(\frac{S_0}{P_{cr}}\right) - C_2^3 C_8 EA_s \frac{(qL)^2}{P_{cr}^3}. \end{aligned} \quad (15)$$

In Equation (14),  $S_{eff}$  is the only unknown and represents the root of a third degree polynomial. The solution is known in literature as Cardano's formula [13,14]. First, the following parameters need to be defined:

$$\begin{aligned} c_P &= A_1/A_3 - (A_2/A_3)^2/3 \\ c_Q &= A_0/A_3 - A_1 A_2/(3A_3^2) + 2[A_2/(3A_3)]^3 \\ c_D &= (c_Q/2)^2 + (c_P/3)^3 \\ c_R &= \sqrt{(c_Q/2)^2 + |c_D|} \\ c_T &= \arccos(-c_Q/2c_R). \end{aligned} \quad (16)$$

Aiming at the desired root among the three available solutions and assuming  $S_{eff}/P_{cr} > -1$ , it can be summarized based on previous parameters as

In this approximation,  $S_{eff}$  was considered constant along the pipe, so the variation due to self-weight was not accounted for, wherefore the calculated value will be that corresponding to the mid-span section.

### 2.3 Complementary Formulae

Once  $S_{eff}$  is known, as mentioned in Section 1, the code DNV-RP-F105 [8] provides simplified formulae to calculate the maximum static moment  $M$  and the deflection  $\delta$ .

$$\begin{aligned} M &= C_5 qL^2 / (1 + S_{eff}/P_{cr}) \\ \delta &= C_6 qL^4 / [EI(1 + S_{eff}/P_{cr})] \end{aligned} \quad (18)$$

where the coefficients  $C_5$  and  $C_6$  are listed in Table 2. In case these formulae do not have enough accuracy, the maximum deflection and momentum can be calculated from the analytical solutions of Equation (3) for a given  $S_{eff}$ . For example, for fixed-fixed condition, the analytical solution of maximum moment will be:

$$M = \begin{cases} \frac{q}{2k^2} \left[ 2 - \frac{kL}{\tanh(kL/2)} \right] & ; \text{ if } S_{eff} > 0 \\ qL^2/12 & ; \text{ if } S_{eff} = 0 \\ \frac{q}{2k^2} \left[ \frac{kL}{\tan(kL/2)} - 2 \right] & ; \text{ if } S_{eff} < 0 \end{cases} \quad (19)$$

where  $k^2 = |S_{eff}| / EI$ .

These equations will be used, based on the  $S_{eff}/P_{cr}$  value calculated in Equation (17), in order

to expand the utility of the proposed formulation. The values obtained will also be compared to numeric results. The natural frequencies will not be evaluated in this work.

The effect of soil flexibility on shoulders could be taken in account by the concept of effective length  $L_{eff}$ , presented by Hobbs [15], that is calculated based on soil stiffness, pipe bending stiffness  $EI$  and span length  $L$ . This approach would bring the proposed solution closer to the real phenomenon.

### 2.4 Design Sequence

For a design procedure, the effective tension at installation position  $S_I$  can be assumed equal to the lay tension  $H_0$ . Then, Equation (14), reformulated to determine  $S_0$  for a given  $S_{eff}$ , can be used to obtain the associated undeformed effective tension  $S_{I_0}$  (Fig. 2a):

$$\left(\frac{S_0}{P_{cr}}\right) = \left(\frac{S_{eff}}{P_{cr}}\right) - \frac{C_8 EA_s (qL)^2}{P_{cr}^3} \left[ C_7 \left(\frac{S_{eff}}{P_{cr}}\right) + \frac{24}{C_2 \pi^2} \right]^{-2} \quad (20)$$

The undeformed effective tension for hydrotest ( $S_{H_0}$ ) and operation ( $S_{O_0}$ ) conditions are calculated adding the temperature and internal pressure increment effect according to the Equation (2).

Finally, Equation (17) is used to calculate the corresponding effective tensions  $S_H$  and  $S_O$  (Fig. 2b and c).

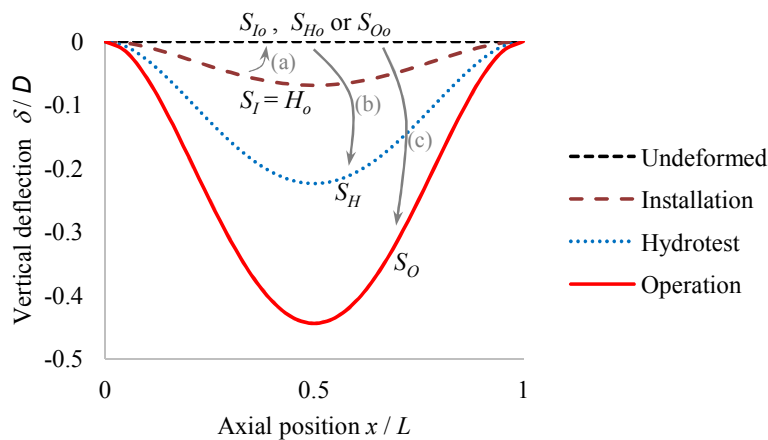


Fig. 2. Example of design sequence for the fixed-fixed condition

### 3. FINITE ELEMENT ANALYSIS

In order to evaluate the accuracy of the proposed solution, a finite element model was implemented in the software ANSYS Mechanical v17, whose structural matrices are derived based on the principle of virtual work. The chosen element type was the PIPE289, which is a quadratic three-node beam element based on Timoshenko's beam theory, that includes first order shear deformation effects and handles large strain and/or rotation nonlinear applications. Because of the limitation of the first order shear deformation theory, the reliability of this element is limited to pipes with slenderness ratios greater than 30 [16]. In this work, the minimum value of the slenderness ratio calculated was 1350, remaining inside the applicability range of the referred formulation. The free span was discretized into elements whose length was set to half de pipe diameter.

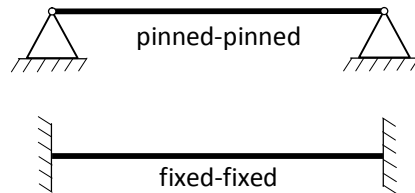


Fig. 3. Boundary condition configurations

Regarding the boundary conditions, for the pinned-pinned configuration, the line end translations were restrained in all three directions and, in order to avoid numerical instability, also in the beam axial rotation. For the fixed-fixed configuration, the line ends were restrained to translate and rotate in all directions.

A distributed vertical load was applied downwards along the pipe, corresponding to the submerged weight. In addition, an internal pressure was defined. The initial effective tension  $S_0$  for each case, calculated by Equation (2), was applied by an imposed axial displacement at one of the ends.

Because of the slenderness of the problem, the simulation was performed considering geometrical nonlinearity, which is calculated based on the Newton-Raphson method. All applied loads, except for the self-weight, were divided into 10 steps, in order to guarantee better convergence and accuracy.

The effective tension result is provided as an output solution from the selected element type.

The value considered for the comparison with the proposed solution is that related to the mid-span section. The maximum moment is obtained by the integration of axial stresses at the mid span section for the pinned-pinned configuration and by the moment reaction at the pipe ends for the fixed-fixed configuration. The maximum deflection corresponds to the vertical displacement at the mid-span.

### 4. RESULTS AND DISCUSSION

#### 4.1 Input Data

The verification cases were generated varying the aimed  $S_{eff}/P_{cr}$  values between -0.5 and 1.0. Values lower than -0.5 became too close to the critical buckling load and, therefore, unlikely to occur for normal pipeline design conditions. On the other hand, values greater than 1.0 are too large for spans with acceptable lengths. The length values were considered from  $L/D = 40$ , increasing this ratio progressively in steps of 20 until the mid-span deflection reached  $12D$ . This limit was chosen in order to remain within realistic design conditions. A total of 140 cases were analyzed.

The pipe properties used are listed in Table 3.

Table 3. Input data for the verification cases

Description	Symbol	Value	Unit
Outer diameter	$D$	457.20	mm
Thickness	$t$	28.575	mm
Young modulus	$E$	207	GPa
Poisson coefficient	$\nu$	0.3	
Steel density	$\rho_s$	7,850	kg/m <sup>3</sup>
Submerged weight	$q$	2.576	kN/m
Internal pressure increment	$\Delta p_i$	28.75	MPa

The initial effective tension  $S_0$  for each desired  $S_{eff}/P_{cr}$  condition is calculated by Equation (20). For the finite element model, Equation (2) is also used to calculate the equivalent displacement that will give the necessary initial tension. Then, after sagging, equilibrium  $S_{eff}$  values calculated in FEA are compared with those provided by the proposed solution, described in Section 2.2.

#### 4.2 Comparison between Results from the Proposed and the Numerical Solutions

This section has been prepared to show the accuracy of the equation proposed in this paper comparing its results with those calculated using

numerical solutions. These results are obtained varying the relative span lengths  $L/D$  and the effective tensions  $S_{eff}/P_{cr}$ . Fig. 4 presents the difference between  $S_{eff}$  values relative to  $P_{cr}$ . Considering all the analysed cases, the maximum relative deviation of estimated  $S_{eff}$  is -2,1 %, which was obtained for  $L/D = 260$  and  $S_{eff}/P_{cr} \cong 1.00$  in the fixed-fixed configuration. In the same configuration, for a smaller  $L/D$  equal to 140, the relative deviation is smaller than 0.5 % for all values of  $S_{eff}/P_{cr}$ . For the pinned-pinned configuration, higher values of  $S_{eff}/P_{cr}$  resulted in even smaller deviations, however, slightly larger values occur for the fixed-fixed boundary conditions for large  $L/D$  values.

The true axial force was obtained by Equation (1) based on the calculated  $S_{eff}$  value. The maximum relative deviation calculated for the axial force was 0.9 % for  $S_{eff}/P_{cr} = -0.50$  (Fig. 5).

As mentioned in Section 2.3, once  $S_{eff}$  is known, the maximum deflection (Fig. 6) and moment

(Fig. 7) can easily be calculated by the simplified formula given in Equation (18), from DNV-RP-F105 [8]. Regarding the deflections, the larger relative deviation was -3.1 %, calculated for  $L/D = 40$  and  $S_{eff}/P_{cr} = 1$  (Fig. 6). In this case, the simplified formula calculated a 2.042 mm displacement against 2.109 mm from the FEA, which means a very small discrepancy in absolute value and, therefore, can be disregarded. For all other analyzed cases, this deviation was smaller than 2.3 % (in modulus). For almost all cases in the pinned-pinned configuration, no significant difference was observed for deflection deviation, while in the fixed-fixed cases the discrepancy tends to decrease along with  $L/D$  and  $S_{eff}/P_{cr}$  combinations.

The moment calculated from DNV-RP-F105 [8] for the pinned-pinned condition has presented a deviation from the numerical results smaller than 2,5 % (Fig. 7a). Up this point, the resulting deviations of the simplified formula in

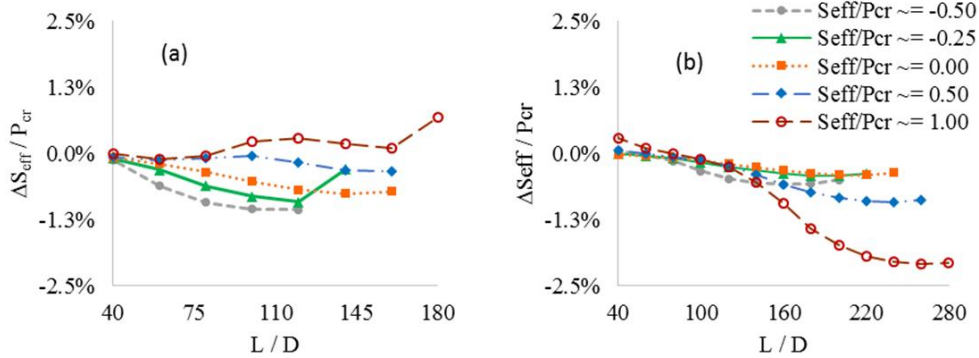


**Fig. 4. Difference between effective tension  $S_{eff}$  calculated by the proposed formulation and by the numerical analyses relative to critical buckling load  $P_{cr}$  for pinned-pinned (a) and fixed-fixed (b) configurations**

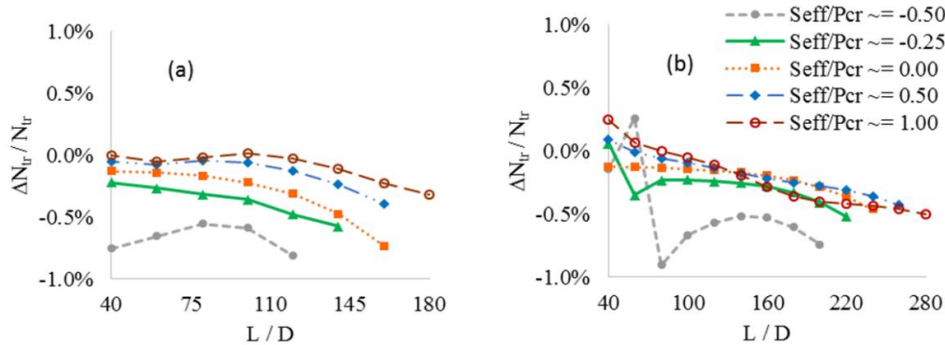


**Fig. 5. Relative difference between the true axial force  $N_{tr}$  calculated by the proposed formulation and in the numerical analysis for the pinned-pinned (a) and fixed-fixed (b) configurations**

Equation (18) are in good agreement with the deviation of the  $S_{eff}$  values calculated based the proposed solution, which is smaller than 3%. This was expected, because those simplified formulae depend on a previously known value of  $S_{eff}$ . However, for the fixed-fixed, the calculated

divergence is much higher (Fig. 7b). This divergence is nearly constant along analyzed  $L/D$  values for each  $S_{eff}P_{cr}$  combination, therefore this formula could be easily adjusted, but it is a third party formula that will not be altered here.

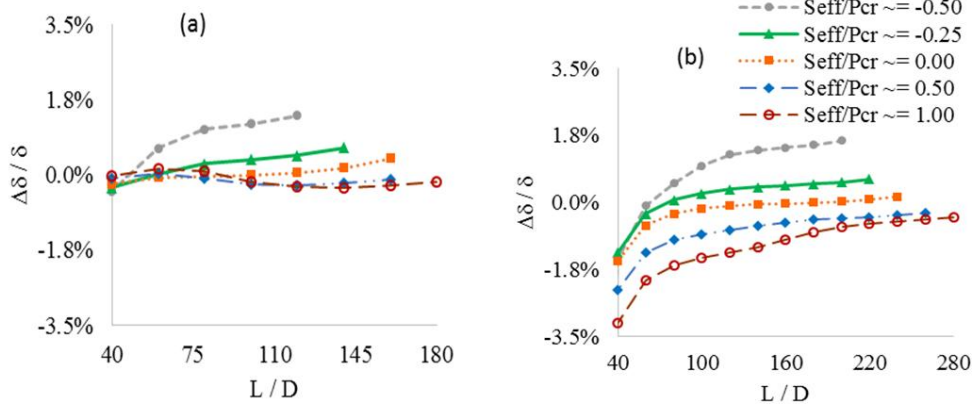


Fig. 6. Relative difference between the deflection  $\delta$  calculated by the DNV-RP-F105 and the numerical analysis for the pinned-pinned (a) and fixed-fixed (b) configurations

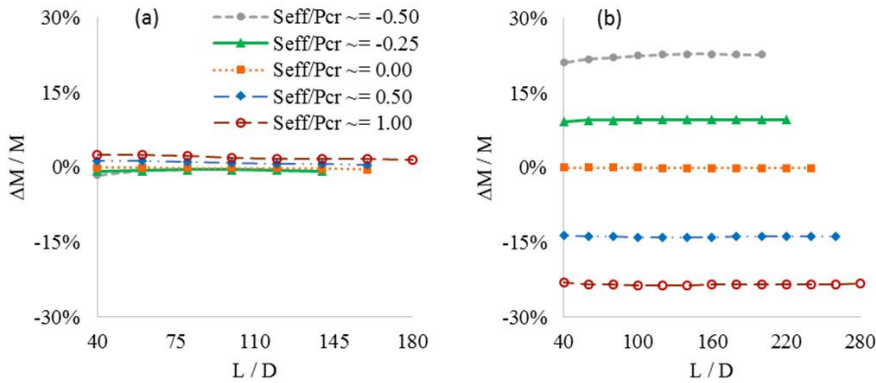


Fig. 7. Relative difference between moment  $M$  calculated by the DNV-RP-F105 and by the numerical analysis for pinned-pinned (a) and fixed-fixed (b) configurations

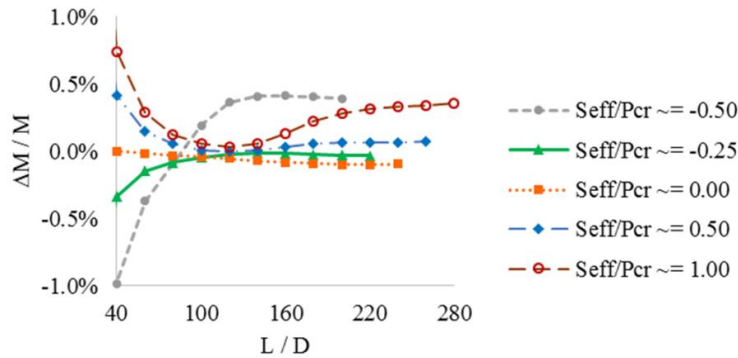
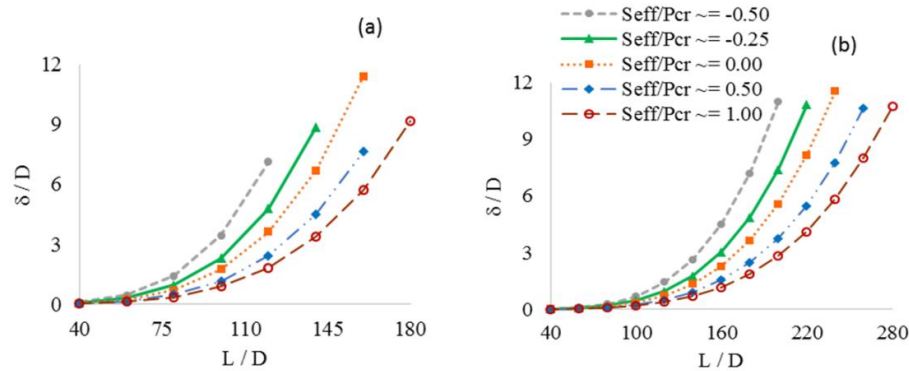


Fig. 8. Relative difference between moment  $M$  calculated by analytical solution and by the numerical analysis for fixed-fixed configurations



**Fig. 9. Maximum deflection  $\delta$  divided by diameter  $D$  calculated by the proposed solution for pinned-pinned (a) and fixed-fixed (b) configurations**

Another way to calculate the moment would be using Equation (19) which was derived here. The results from Equation (19) are plotted in Fig. 8 showing divergence less than 1 % (in modulus) and, therefore, much better than those obtained about with Equation (18).

In Fig. 9 are shown the relative maximum deflection  $\delta/D$ , which calculation was also based on  $S_{eff}$  value from the proposed solution. Since those results are very close to numerical calculation (Fig. 6) there is no need to present those ones too. Maximum values analyzed were  $\delta/D = 11.39$  for pinned-pinned and  $\delta/D = 11.56$  for fixed-fixed condition.

## 5. CONCLUSIONS

Although free spans are common and frequently assessed in submarine pipeline, there is a lack of simple and accurate tools to calculate the effective tension and FEA is usually applied. This value is necessary to calculate many of the important information as true axial force, bending moment, deflection and natural frequency.

The methodology developed in this work is based on an approximated solution and make it possible to derive a straightforward equation to calculate the effective tension  $S_{eff}$  for any practical condition of pressure and temperature.

The results from the proposed solution compared to the numerical solution presented high accuracy. The calculated divergence between those solutions were smaller than 2.1% for relative effective tension ( $S_{eff}/P_{cr}$ ) and smaller than 0.9 % for the axial force (in modulus).

Based on the  $S_{eff}$  values calculated by the proposed solution, the DNV-RP-F105 [8]

simplified equations were used to calculate the maximum deflection and moment. Those results also presented great agreement with the numerical solution, except for the moment in fixed-fixed condition. It has been shown, however, that Equation (19), derived here, is an accurate replacement for the Equation (18) from DNV-RP-F105 [8].

Many different cases were calculated, for pinned-pinned and fixed-fixed condition, varying  $L/D$  from 40 to 280 (limited for relative deflection  $\delta/D < 12$ ) and  $S_{eff}/P_{cr}$  from -0.5 to 1.0. According to those results, the proposed solution appears to be a relatively simple and very accurate tool for free span assessments in any practical condition.

In a future research, the stiffness of the soil on span shoulders could be taken in account in order to develop the same methodology of this work on a more detailed analysis, however, in the meantime, the soil stiffness can be accounted for by the effective length ( $L_{eff}$ ) [15].

## COMPETING INTERESTS

Authors have declared that no competing interests exist.

## REFERENCES

1. Taylor N, Tran V. Prop-imperfection subsea pipeline buckling. Mar Struct. 1993; 6(4):325-358. DOI: 10.1016/0951-8339(93)90001-J
2. Xu J, Li G, Horrillo JJ, Yang R, Cao L. Calculation of maximum allowable free span length and safety assessment of the

- DF1-1 submarine pipeline. J Ocean Univ China. 2010;9(1):1-10.  
DOI: 10.1007/s11802-010-0001-4
3. Palmer AC, Baldry JAS. Lateral Buckling of Axially Constrained Pipelines. J Pet Technol. 1974;26(11):1283-1284.  
DOI: 10.2118/4815-pa
  4. Sparks CP. The influence of tension, pressure and weight on pipe and riser deformations and stresses. J Energy Resour Technol. 1984;106(1):46.  
DOI: 10.1115/1.3231023
  5. Galgoul NS, Massa ALL, Claro CA. Lateral buckling: Trying to be less conservative. In: 2004 International Pipeline Conference, Volumes 1, 2, and 3. Calgary, Alberta, Canada: ASME. 2004;1899-1904.  
DOI: 10.1115/ipc2004-0334
  6. Fyrileiv O, Collberg L. Influence of Pressure in Pipeline Design: Effective Axial Force. In: 24th International Conference on Offshore Mechanics and Arctic Engineering: Volume 3. Halkidiki, Greece: ASME. 2005;629-636.  
DOI: 10.1115/OMAE2005-67502
  7. Vedeld K, Sollund HA, Hellesland J, Fyrileiv O. Effective axial forces in offshore lined and clad pipes. Eng Struct. 2014;66: 66-80.  
DOI: 10.1016/j.engstruct.2014.01.051
  8. Det Norske Veritas. DNV-RP-F105: Free spanning pipelines. 2006;1-46.
  9. Hobbs RE. Pipeline buckling caused by axial loads. J Constr Steel Res. 1981;1(2):2-10.  
DOI: 10.1016/0143-974X(81)90027-4
  10. Hobbs RE. In-Service Buckling of Heated Pipelines (PDF Download Available).pdf. ASCE J Transp Eng. 1984;110(2):175-189.  
DOI:10.1061/(ASCE)0733-947X(1984)110:2(175)
  11. Vedeld K, Sollund H, Hellesland J. Free vibrations of free spanning offshore pipelines. Eng Struct. 2013;56:68-82.  
DOI: 10.1016/j.engstruct.2013.04.013
  12. Sollund HA, Vedeld K, Fyrileiv O. Modal response of short pipeline spans on partial elastic foundations. Ocean Eng. 2015;105: 217-230.  
DOI:<http://dx.doi.org/10.1016/j.oceaneng.2015.06.019>
  13. Van der Waerden BL. A history of algebra: from Al-Khwarizmi to Emmy Noether. 1st ed. Springer Berlin Heidelberg; 1985.  
Available:<https://books.google.com.br/books?id=W6DwCAAQBAJ>
  14. Irving R. Beyond the quadratic formula. Mathematical Association of America; 2013.  
Available:[https://books.google.com.br/books?id=CV\\_UInCRO38C](https://books.google.com.br/books?id=CV_UInCRO38C)
  15. Hobbs RE. Influence of structural boundary conditions on pipeline free span dynamics. In: 5th International Symposium on Offshore Mechanics and Arctic Engineering. ASME. 1986;685-691.
  16. ANSYS Mechanical, Release 17. 2016.

© 2018 Nascimento and Szilard; This is an Open Access article distributed under the terms of the Creative Commons Attribution License (<http://creativecommons.org/licenses/by/4.0>), which permits unrestricted use, distribution, and reproduction in any medium, provided the original work is properly cited.

*Peer-review history:*

*The peer review history for this paper can be accessed here:  
<http://www.sciencedomain.org/review-history/23855>*